INORGANIC CHEMISTRY
FRONTIERS

RESEARCH ARTICLE

View Article Online
View Journal | View Issue

Cite this: *Inorg. Chem. Front.*, 2023, **10**, 591

A ferrocene-containing analogue of the MCU inhibitor Ru265 with increased cell permeability†

Zhouyang Huang, Jesse A. Spivey, Samantha N. MacMillan and Justin J. Wilson *

The mitochondrial calcium uniporter (MCU) is a transmembrane protein that mediates mitochondrial calcium (mCa^{2+}) uptake. Inhibitors of the MCU are of interest for their applications as tools to study the role of mCa^{2+} uptake on cellular function. In this study, we report two potent MCU inhibitors, $[Ru_2(\mu\text{-}N)(NH_3)_8(FcCO_2)_2](OTf)_3$ (**RuOFc**, Fc = ferrocene, OTf = triflate) and $[Ru_2(\mu\text{-}N)(NH_3)_8(PhCO_2)_2](OTf)_3$ (**RuOBz**). These compounds are analogues of the previously reported inhibitor $[Ru_2(\mu\text{-}N)(NH_3)_8(Cl)_2](Cl)_3$ (**Ru265**) that has been derivatized with ferrocenecarboxylate and benzoate ligands, respectively. Both compounds were synthesized and fully characterized by NMR spectroscopy, infrared spectroscopy and X-ray crystallography. Under physiological conditions, **RuOFc** and **RuOBz** aquate with half-lives of 2.9 and 6.5 h, respectively, to produce $[Ru_2(\mu\text{-}N)(NH_3)_8(H_2O)_2](OTf)_5$ (**Ru265'**) and the free carboxylates. Cyclic voltammetry of **RuOFc** in *N*,*N*′-dimethylformamide (DMF) reveals a prominent reversible 2e$^-$ transfer event at 0.64 V *vs.* SCE, corresponding to the simultaneous oxidation of both ferrocene-containing axial ligands. All three complexes also exhibit irreversible Ru-based reductions at potentials below –1 V *vs.* SCE. DFT calculations of **Ru265'**, **RuOFc** and **RuOBz** confirm that the redox activity of **RuOFc** arises from the ferrocene ligands. Furthermore, LUMO energies of the three compounds correlate with their irreversible reduction potentials. A systematic comparison on the biological properties of **Ru265**, **RuOFc** and **RuOBz** was carried out. Both **RuOFc** and **RuOBz** inhibit mCa^{2+} uptake in permeabilized HEK293T cells, but are 5–7 fold less potent than **Ru265**. In intact cells, **RuOBz** is taken up by cells and inhibits the MCU to a similar extent as Ru265. **RuOFc**, however, exhibits a 10-fold increase in cellular uptake over **Ru265**, which in turn also leads to a modest enhancement in MCU-inhibitory activity in intact cells. Moreover, in contrast to **Ru265**, **RuOFc** is cytotoxic to HEK293T and HeLa cells with 50% growth inhibitory concentration values of 23.2 and 33.9 μM, respectively, a property that could be leveraged to develop MCU-targeting anticancer agents. These results establish **RuOFc** as a potent MCU inhibitor and another example of how axial ligand functionalization of **Ru265** can lead to new compounds within this class with diverse physical and biological properties.

Received 10th October 2022,
Accepted 30th November 2022

DOI: 10.1039/d2qi02183h

rsc.li/frontiers-inorganic

Introduction

Mitochondrial calcium (mCa^{2+}) plays an important role in a wide range of biological processes that are critical for cellular function.[1,2] The uptake of mCa^{2+} is enforced by the mitochondrial calcium uniporter (MCU), a highly selective inwardly rectifying Ca^{2+} channel.[3–5] Elevated mCa^{2+} levels are associated with a wide range of pathological conditions,[6,7] including ischemia-reperfusion injury,[8,9] cancer,[10–12] and neurodegenerative disorders.[13–16] Given the involvement of mCa^{2+} in these human diseases, there has been a growing interest in developing compounds that can inhibit the MCU to prevent mCa^{2+} overload.[17,18]

The dinuclear oxo-bridged ruthenium compound, **Ru360** (Chart 1), is among the most well-known MCU inhibitors.[19–21] However, the therapeutic use of this compound is limited by its low cell permeability and redox instability. Several other Ru-based MCU inhibitors have been reported,[22,23] including a nitrido-bridged analogue of **Ru360**, named **Ru265** (Chart 1).[24] Unlike the mixed valent complex **Ru360** (Ru^{3+}/Ru^{4+}), **Ru265** contains two Ru^{4+} centers. This compound is cell permeable and stable toward biological reduction, enabling it to inhibit mCa^{2+} uptake in non-permeabilized cells. This latter property was leveraged to demonstrate protective effects against oxygen-glucose deprivation in cortical neurons *in vitro* and an *in vivo* mouse model of ischemic stroke.[25] Under physiological con-

Department of Chemistry and Chemical Biology, Cornell University, Ithaca, New York 14853, USA. E-mail: jjw275@cornell.edu

†Electronic supplementary information (ESI) available. CCDC 2212058 and 2212059. For ESI and crystallographic data in CIF or other electronic format see DOI: https://doi.org/10.1039/d2qi02183h

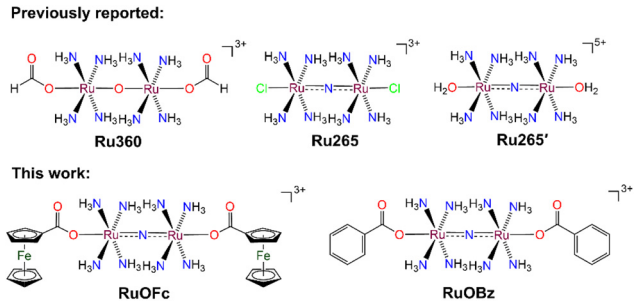

Chart 1 Structures of Ru-based MCU inhibitors.

ditions, **Ru265** aquates on the timescale of minutes to afford the diaqua-capped species **Ru265′** (Chart 1). Based on the rapid aquation of **Ru265**, **Ru265′** is presumed to be the active MCU inhibitor.[26,27] Mutagenesis and molecular docking studies have suggested that **Ru265′** inhibits mCa^{2+} uptake through interaction with the exposed DIME peptide sequence region of the MCU pore.[28]

Recently, we reported that **Ru265** can be modified by swapping its axial chloride ligands with carboxylates.[29] Notably, the carboxylate-capped analogues aquate under physiological conditions with half-lives on the order of hours, a timescale that is significantly longer than that of the chloride-capped **Ru265**. We further demonstrated that the MCU-inhibitory properties of these carboxylate-capped compounds increase over time as the aquation reaction proceeds, suggesting that they act as potential aquation-activated prodrugs for **Ru265′**. Despite their prolonged stability, the short alkyl chain carboxylate-capped prodrugs do not exhibit an enhancement of cellular uptake compared to **Ru265**. Recognizing the importance of this prodrug approach for developing new analogues of **Ru265**, we sought to employ more lipophilic axial ligands to access candidates with improved cell permeability.[30–33]

Among the different potential axial ligands, we considered ferrocenecarboxylate because prior studies have shown that the introduction of ferrocene into drug candidates can substantially enhance their lipophilicity, as well as confer them with therapeutically useful redox activity.[34–36] Two key examples of the success of this strategy are found in the antimalarial drug candidate ferroquine[37,38] and the anticancer agent ferrocifen.[39] These drug candidates are ferrocene-containing derivatives of the antimalarial drug chloroquine and chemotherapeutic agent tamoxifen, respectively. Importantly, the enhanced lipophilicity afforded by the ferrocene group leads to greater parasite uptake of ferroquine[40,41] and higher tumor cell uptake by ferrocifen,[42,43] contributing to their higher potencies than the parent drugs. Furthermore, their redox-activities also give rise to reactive oxygen species that further improves their potency.[44–47] It is also worth noting that a number of heteronuclear ruthenium–ferrocene complexes have been investigated for their anticancer properties.[48] The mechanisms of action of these complexes are case-dependent,[34] but it has been demonstrated that the presence of the ferrocene group typically potentiates the formation of cytotoxic reactive oxygen species and facilitates cellular uptake.[48] Inspired by these and many other ferrocene-derivatized drug candidates, in this study we investigated the physical and biological properties of a ferrocenecarboxylate-capped **Ru265** analogue, named **RuOFc** (Chart 1), demonstrating it to be a potent cell-permeable MCU inhibitor.

Results and discussion

Synthesis and characterization

RuOFc was synthesized using a strategy similar to the one that was employed to prepare the alkyl carboxylate derivatives of **Ru265**.[29] Briefly, the axial chlorides on **Ru265** were removed as insoluble AgCl by treating the compound with 5 equiv. of AgOTf in water to afford the diaqua-capped **Ru265′**. This synthon was allowed to react with sodium ferrocenecarboxylate to obtain **RuOFc**. Given that ferrocene has been frequently used as a bioisostere for phenyl or heteroaromatic rings in drugs due to their structural similarities,[34] we also synthesized the benzoate-capped derivative of **Ru265** (**RuOBz**, Chart 1) as a redox-inactive analogue of **RuOFc**. Both **RuOFc** and **RuOBz** were characterized by various methods (Fig. S2–S8 and Table S1†), including NMR spectroscopy, infrared (IR) spectroscopy, HPLC and X-ray crystallography. The ^{1}H NMR spectra of **RuOFc** and **RuOBz** exhibit a broad resonance assigned to the protons of the NH_3 ligands at 4.03 and 4.08 ppm (Fig. S2 and S4†), respectively. These chemical shifts are upfield of those of **Ru265**, for which the NH_3 resonance appears at 4.15 ppm.[24] This result suggests the axial oxygen donors increase the shielding of the equatorial ammine protons, a property that was previously observed in the alkyl carboxylate-capped **Ru265** analogues. The ^{13}C{^{1}H} NMR spectra of both complexes reveal expected resonances of the carboxylate ligands and triflate counterions (Fig. S3 and S5†). Likewise, the ^{19}F NMR spectra of both compounds reveal a single peak at −77.7 ppm that is assigned to the triflate counterions (Fig. S6†). The IR spectra of **RuOFc** and **RuOBz** exhibit intense peaks at 1023 and 1026 cm^{-1}, respectively, which correspond to the asymmetric Ru–N–Ru stretching modes arising from the bridging nitrido ligand (Fig. S7†). These energies are significantly lower than that of **Ru265**, which appears at 1046 cm^{-1}. Collectively, these spectroscopic data support the characterization of **RuOFc** and **RuOBz**. With respect to their lipophilicities, the addition of ferrocenecarboxylate and benzoate ligands is expected to enhance this property relative to **Ru265**. Accordingly, RP-HPLC analysis of **RuOFc** and **RuOBz** reveals these compounds to exhibit significant retention on the reverse-phase C18 column used (Fig. S8†). By contrast, **Ru265** elutes within the dead time of the column, showing no retention. Because compound retention on RP-HPLC systems correlates with the lipophilicity of metallodrug candidates,[49–51] these results indicate that **RuOFc** and **RuOBz** are significantly more lipophilic than **Ru265**. The quantitative logarithm values of n-octanol–water partition coefficients (log P) of **RuOFc** and

RuOBz could be obtained after creating a calibration curve of retention factors *versus* known log *P* values of other compounds (Fig. S9 and S10†).[52] Using the easily measured HPLC retention factors along with this calibration curve, the log *P* values of **RuOFc** and **RuOBz** were determined to be 2.0 and 0.6, respectively, indicating that the ferrocene group has a larger effect on compound lipophilicity (Table 1). This result is consistent with the greater log *P* value of ferrocene (2.66)[34] compared to benzene (2.13).[53]

X-ray crystallography

The crystal structures of **RuOBz** and **RuOFc** reveal the expected molecular geometries, showing the $Ru(NH_3)_4(\mu\text{-}N)Ru(NH_3)_4$ core with two carboxylates on the axial positions (Fig. 1). For **RuOBz**, the bridging nitrogen atom resides on a crystallographic inversion center, affording this complex with C_i symmetry and a perfectly linear Ru–N–Ru angle. In contrast, the Ru–N–Ru motif in **RuOFc** slightly deviates from linearity with an angle of 175.4(2)°. For both complexes, the Ru–N distances, 1.740(3) Å for bridging nitrogen atoms and 2.098(5)–2.17(1) Å for equatorial nitrogen atoms and Ru–O distances, 2.091(2)–2.104(2) Å (Table S2†), are similar to those previously observed for the formate- and propionate-capped analogues of **Ru265**.[29] A comparison of the average axial Ru–O distances of **RuOFc** and **RuOBz** reveals them to be indistinguishable within the error of the measurement (Table 1). This result suggests that the donor strengths of these two axial carboxylates are not substantially different, a property that would be predicted based on the identical pK_a values of their conjugate acids (Table 1). The equatorial ammine ligands in **RuOBz** are arranged in an eclipsed conformation about the Ru–N–Ru vector, whereas in **RuOFc** they are staggered. Because molecular orbital interactions do not require a particular arrangement of these ammines, the difference in conformation between these two complexes is most likely a consequence of solid-state packing interactions. For other octaammine nitrido-bridged complexes that have been crystallized, both staggered and eclipsed conformations have been observed, further supporting the small energetic differences between these states and their potential sensitivity to solid-state interactions.[24] In addition, the axial carboxylates intramolecularly hydrogen bond with the equatorial ammines in both compounds, an interaction that has been observed in other carboxylate-capped **Ru265** analogues[29] as well as Pt(IV) ammine complexes with carboxylate ligands.[54] Lastly, the Fe–$Cp_{centroid}$ distances in **RuOFc** span from 1.6423(15) to 1.648(2) Å. These values are not substantially different from those found in the crystal structure of free ferrocenecarboxylic acid[55] (1.636(5) and 1.639(4) Å), suggesting that coordination to Ru does not significantly perturb the structures of and bonding within these ferrocene moieties.

Table 1 Relevant physical properties of **RuOBz** and **RuOFc**

Property	**RuOBz**	**RuOFc**
Aquation rate constant k ($\times 10^5$ s^{-1})	3.0 ± 0.3	6.8 ± 0.6
$t_{1/2}$ (h)	6.5 ± 0.7	2.9 ± 0.3
pK_a [a]	4.20[b]	4.20[c]
Average Ru–O (Å)	2.099	2.098
Redox events (V *vs.* SCE)	−1.27	0.64, −1.35
Log *P*	0.6	2.0

[a] pK_a of the conjugate acids of the free ligands. [b] Ref. 56. [c] Ref. 57.

Physical properties

Having established the identity and purity of the two compounds, we proceeded to examine their stability under physiological conditions by UV-vis spectroscopy (Fig. 2 and S11†). The spectral changes over time were fit using a first-order kinetic model for a single-step reaction to obtain rate constants and half-lives for this process (Table 1). Even though the aquation of these compounds should proceed *via* a two-step process with a monosubstituted intermediate, UV-vis spectroscopy is unable to resolve both steps, presumably due to the minimal presence of the mono-carboxylate intermediate and its spectral overlap with other species in the solution. As such, the pseudo-first-order rate constants obtained *via* UV-vis spectroscopy represent the rate-determining loss of the first carboxylate ligand.[26,27,29] The aquation half-lives in pH 7.4 buffer at 37 °C for **RuOBz** and **RuOFc** are 6.5 and 2.9 h, respectively, within the range of other carboxylate-capped **Ru265** complexes whose half-lives span 3.3–9.9 h.[29] Notably, the aquation rate constant of **RuOFc** is approximately two times greater than that of **RuOBz**, despite the fact that the axial Ru–O distances within these complexes are indistinguishable and the donors strengths of ferrocenecarboxylate and benzoate are similar, as reflected by the pK_a values of their conjugate acids (Table 1). The faster aquation kinetics of **RuOFc** may therefore be a con-

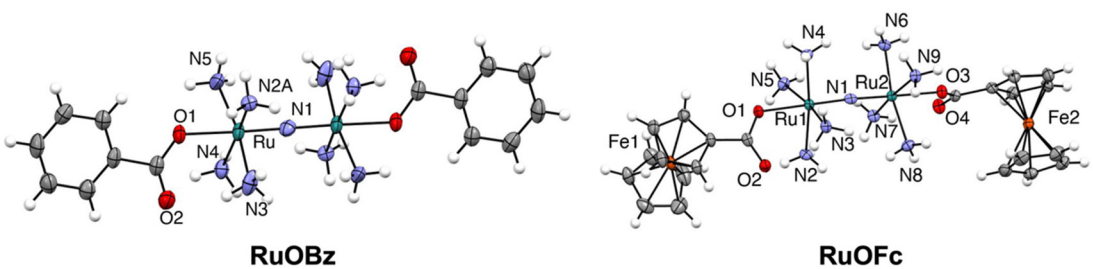

Fig. 1 Crystal structures of **RuOBz** and **RuOFc**. Thermal ellipsoids are shown at the 50% probability level. Solvents and counterions are omitted for clarity.

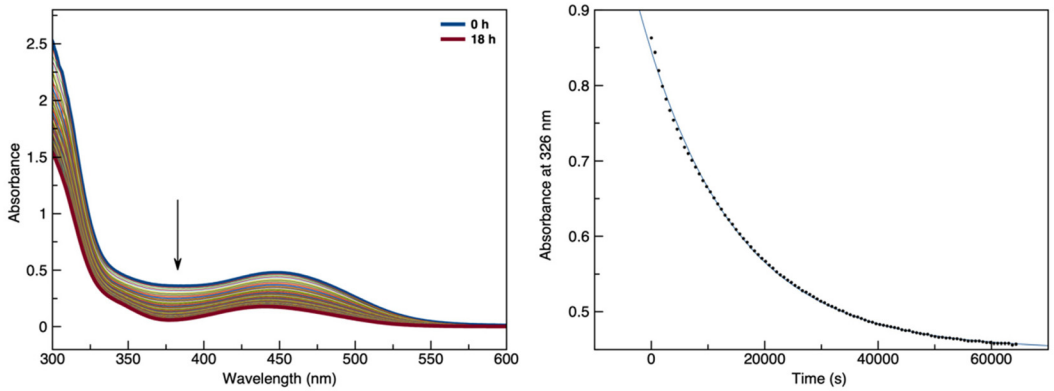

Fig. 2 Left: evolution of the UV-vis spectrum of **RuOFc** (160 μM) in pH 7.4 MOPS-buffered (16 mM) aqueous solution over an 18 h period at 37 °C. Right: Plot of absorbance at 326 nm *versus* time with the best exponential fit.

sequence of a lower energy transition state, rather than a difference in the thermodynamic ground states of the complexes.

Given the redox activity of ferrocene,[58] we examined the electrochemical properties of the complexes by cyclic voltammetry (Fig. 3 and Table 1). In contrast to **Ru265′** and **RuOBz**, which are not redox-active within the biological window, **RuOFc** exhibits a prominent reversible redox event at 0.64 V *vs.* SCE, which is assigned to the ferrocene/ferricenium redox couple. This value is lower than that of free ferrocenecarboxylic acid, which occurs at 0.79 V *vs.* SCE (Fig. S12†), indicating that coordination to **Ru265** impacts the redox potential of this fragment. Furthermore, the peak-to-peak separation of this event is approximately 30 mV, revealing it to be a two-electron transfer process.[59] This result suggests that both ferrocenecarboxylate ligands are oxidized simultaneously and implies that the mixed-valent mono-oxidized compound is thermodynamically unstable, presumably due to the large separation and poor electronic communication between the two ferrocenes on **RuOFc**.[60,61] In addition to this reversible ferrocene-based redox event, an irreversible redox event around −1 V is observed for all three compounds, which is assigned to the reduction of the ruthenium centers. In previous electrochemical studies of **Ru265** in aqueous solutions, this feature was not observed, presumably due to the smaller accessible potential window within water.[26,59] Both **RuOBz** and **RuOFc** have more negative reduction potentials of −1.27 V and −1.35 V, respectively, than **Ru265′** (−1.07 V). The more negative redox potentials of these compounds are consistent with the electrochemical Lever parameters of carboxylates compared to water,[62,63] which reflect the greater donor strength of these carboxylate ligands.

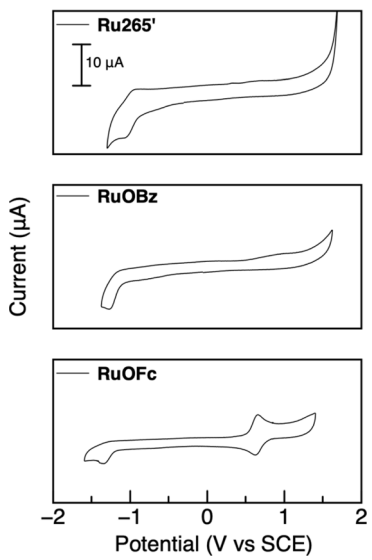

Fig. 3 Cyclic voltammograms of **Ru265′**, **RuOBz** and **RuOFc** in DMF with 0.1 M $[Bu_4N][PF_6]$ (TBAP) at 25 °C and 0.1 V s^{-1} scan rate.

Computational studies

To gain a deeper understanding of the electronic structures of the compounds, we performed DFT calculations on **Ru265′**, **RuOBz** and **RuOFc**. The geometries of these complexes were optimized starting from the coordinates obtained experimentally *via* X-ray crystallography and the energies and compositions of their frontier molecular orbitals were compared (Fig. 4). The HOMO of **Ru265′** and **RuOBz** and HOMO-10 of **RuOFc** are π* molecular orbitals between the axial carboxylate ligands and ruthenium centers. Within **RuOFc** and **RuOBz**, these orbitals are higher energy than that of the **Ru265′**, reflecting the stronger π-donating interaction[64] of these carboxylates compared to water. Notably, the HOMO of **RuOFc** is a ferrocene-based bonding orbital. This high-lying HOMO is the redox-active orbital of **RuOFc**, conferring it with the observed reversible redox event at 0.64 V *vs.* SCE. The LUMO of all three compounds is a delocalized π* orbital between the nitrido bridge and two ruthenium centers. The relative energies of LUMO correlate with the ease of reduction, as measured by cyclic voltammetry. Compared to **Ru265′**, **RuOBz** and **RuOFc** have higher LUMO energies and more negative Ru reduction potentials due to the higher donor strength of the carboxylates.

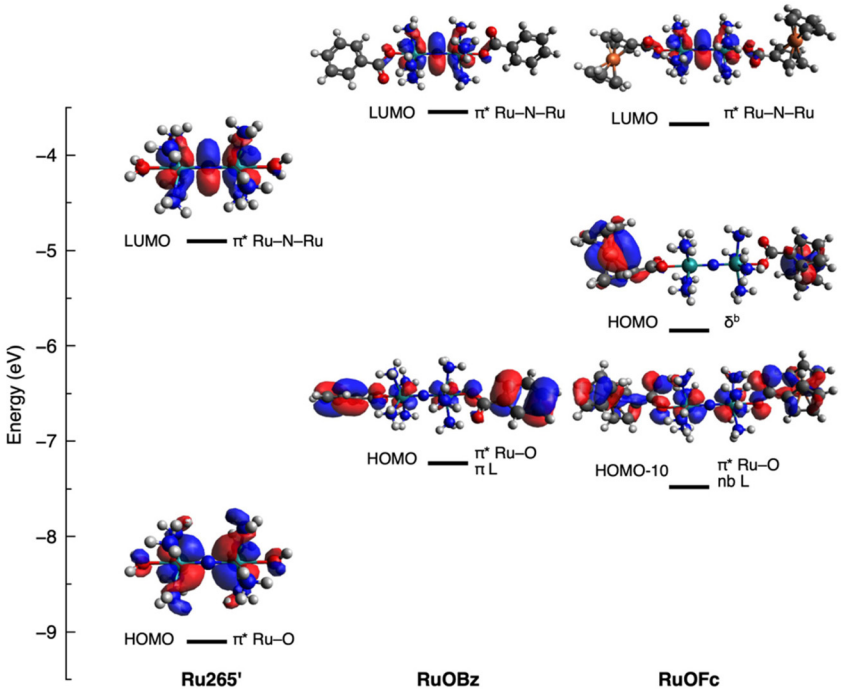

Fig. 4 Frontier Kohn–Sham molecular orbital diagrams of **Ru265'**, **RuOBz** and **RuOFc** drawn with an isovalue of 0.02.

Biological properties

We next evaluated the biological activity of these compounds (Table 2). Both **RuOBz** and **RuOFc** inhibit mCa^{2+} uptake in permeabilized HEK293T cells with nanomolar 50% inhibitory concentration (IC_{50}) values (Table 2 and Fig. S14–S16†). These compounds, however, are 5–7 fold less active than **Ru265**, indicating that the carboxylate ligands reduce the mCa^{2+} uptake-inhibitory properties of these complexes, as previously observed.[29] Next, we examined the cellular uptake of these compounds in HEK293T cells (Table 2). **RuOBz** and **Ru265** exhibit similar cell uptake, whereas **RuOFc** accumulates in 10-fold higher levels. Similar cellular uptake levels were found in HeLa cells treated under identical conditions, indicating that the ability of **RuOFc** to be internalized effectively occurs in different cell lines (Table S3†). The dramatic improvement in cell permeability is most likely facilitated by the high lipophilicity of the ferrocene functional group. The inclusion of ferrocene on other drug candidates has likewise led to increases in cellular uptake.[36,40,41,65,66] If **RuOFc** were to undergo aquation before being internalized, we would expect to its levels in cells to be equivalent to those of **Ru265**, which aquates over the time course of minutes. Therefore, this result also implies that the rate of cellular uptake is faster than the rate of aquation of **RuOFc**, which enables this compound to be taken up in its intact, more lipophilic form. Encouraged by the excellent cell permeability, we determined the ability of these compounds to inhibit mCa^{2+} in intact, non-permeabilized cells (Fig. 5). The mCa^{2+} dynamics in HeLa cells in the presence and absence of **RuOFc** and **RuOBz** were monitored using the mitochondria-localizing Ca^{2+}-responsive Rhod2AM fluorescent sensor.[67] Histamine was added to stimulate mCa^{2+} uptake and the degree of mCa^{2+} uptake was measured by analyzing the fluorescence increase (F/F_0) of the Rhod2AM sensor. As shown in Fig. 5, **RuOBz** is able to inhibit mCa^{2+} uptake in intact cells to a comparable extent as **Ru265**. By contrast, **RuOFc** exhibits a modest yet statistically significant increase in inhibitory activity compared to **Ru265**, a property that may be a consequence of its enhanced cellular uptake. Lastly, to verify that these compounds do not negatively affect mitochondrial function, we performed the JC-1 assay to probe the integrity of the mitochondrial membrane potential (Fig. S17†). In comparison to the positive control carbonyl cyanide m-chlorophenyl hydrazine (CCCP), these compounds do not lead to depolarization of the mitochondrial membrane potential in HeLa cells, when incubated at 50 μM concentration for 24 h. Collectively, these results highlight the promise of using these compounds as MCU inhibitors in intact cells. To confirm that the compounds do not adversely affect cell viability, we examined the cytotoxic effects of the compounds in cells by the 3-(4,5-dimethylthiazol-2-yl)-2,5-tetrazolium bromide (MTT) assay (Table 2 and Fig. S13†). Unexpectedly, in contrast to all other **Ru265** analogues including **RuOBz**, **RuOFc** exhibits moderate cytotoxicity

Table 2 Relevant biological properties of **Ru265**, **RuOBz** and **RuOFc** in HEK293T cells

Property	Ru265	RuOBz	RuOFc
mCa^{2+} uptake inhibition IC_{50} (nM)[a]	2.2 ± 0.6	13.9 ± 3.5	10.5 ± 3.6
Cytotoxicity IC_{50} (μM)[b]	195 ± 8[c]	>90	23.2 ± 1.9
Cellular uptake (pg Ru/μg protein)[d]	33 ± 7	45 ± 5	382 ± 28

[a] In permeabilized cells. [b] 48 h incubation. [c] Ref. 24. [d] 2 h incubation.

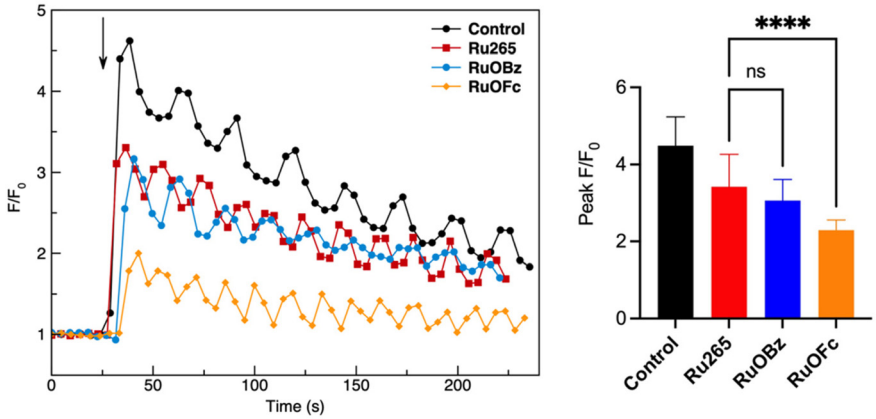

Fig. 5 Left: representative mCa^{2+} uptake after addition of 100 μM histamine in HeLa cells that were pretreated with or without **Ru265**, **RuOBz**, or **RuOFc** (50 μM) for 3.5 h and then loaded with 2 μM Rhod2AM. The arrow indicates the time of histamine addition. Right: Peak F/F_0 in response to the histamine addition. Data represent mean ± standard deviation (SD) ($n > 17$; ****$p < 0.0001$; ns = not significant).

in both HEK293T and HeLa cells with IC_{50} values of 23.2 and 33.9 μM, respectively. Although undesirable for use solely as an MCU inhibitor, this cytotoxicity could potentially be leveraged for using **RuOFc** as an anticancer agent, given the growing interest in targeting the MCU for cancer treatment.[10–12] Ongoing studies are aimed at elucidating the mechanism of action of **RuOFc** and evaluating its anticancer potential.

Conclusions

In summary, two analogues of **Ru265** bearing lipophilic axial carboxylate ligands, **RuOFc** and **RuOBz**, were synthesized and investigated for their biological properties. The inclusion of the benzoate axial ligand in **RuOBz** appears to have no significant effects in terms of altering the biological properties relative to **Ru265**. By contrast, **RuOFc**, which contains axial ferrocenecarboxylate ligands, is substantially more lipophilic than **Ru265** and is accordingly taken up by cells more effectively. These results highlight how axial ligand modification of this class of compounds is an effective approach for tuning the physical and biological properties of **Ru265**-based MCU inhibitors, that is complementary to our recent work showing the effects of altering the metal center.[68] This general functionalization expands the toolkit of MCU inhibitors that can be fine-tuned for specific applications in managing pathological conditions related to dysregulation of mCa^{2+} levels.

Conflicts of interest

The authors declare no competing financial interests.

Acknowledgements

This research was supported by Cornell University and the NSF under award number CHE-1750295. This work made use of the Cornell University NMR facility, which is supported by the NSF under award number CHE-1531632. Additional resources included the use of the Cornell University Biotechnology Resource Center, which is supported by the NIH (NIH S10RR025502).

References

1 M. J. Berridge, M. D. Bootman and H. L. Roderick, Calcium Signalling: Dynamics, Homeostasis and Remodelling, *Nat. Rev. Mol. Cell Biol.*, 2003, **4**, 517–529.
2 D. E. Clapham, Calcium Signaling, *Cell*, 2007, **131**, 1047–1058.
3 Y. Kirichok, G. Krapivinsky and D. E. Clapham, The Mitochondrial Calcium Uniporter Is a Highly Selective Ion Channel, *Nature*, 2004, **427**, 360–364.
4 K. J. Kamer and V. K. Mootha, The Molecular Era of the Mitochondrial Calcium Uniporter, *Nat. Rev. Mol. Cell Biol.*, 2015, **16**, 545–553.
5 N. Nemani, S. Shanmughapriya and M. Madesh, Molecular Regulation of MCU: Implications in Physiology and Disease, *Cell Calcium*, 2018, **74**, 86–93.
6 C. Mammucari, G. Gherardi and R. Rizzuto, Structure, Activity Regulation, and Role of the Mitochondrial Calcium Uniporter in Health and Disease, *Front. Oncol.*, 2017, **7**, 139.
7 D. M. Arduino and F. Perocchi, Pharmacological Modulation of Mitochondrial Calcium Homeostasis, *J. Physiol.*, 2018, **596**, 2717–2733.
8 K. Shintani-Ishida, M. Inui and K. Yoshida, Ischemia-Reperfusion Induces Myocardial Infarction through Mitochondrial Ca^{2+} Overload, *J. Mol. Cell. Cardiol.*, 2012, **53**, 233–239.
9 E. J. Lesnefsky, Q. Chen, B. Tandler and C. L. Hoppel, Mitochondrial Dysfunction and Myocardial Ischemia-Reperfusion: Implications for Novel Therapies, *Annu. Rev. Pharmacol. Toxicol.*, 2017, **57**, 535–565.

10 A. H. L. Bong and G. R. Monteith, Calcium Signaling and the Therapeutic Targeting of Cancer Cells, *Biochim. Biophys. Acta, Mol. Cell Res.*, 2018, **1865**, 1786–1794.
11 A. Vultur, C. S. Gibhardt, H. Stanisz and I. Bogeski, The Role of the Mitochondrial Calcium Uniporter (MCU) Complex in Cancer, *Pflug. Arch. Eur.*, 2018, **470**, 1149–1163.
12 C. Delierneux, S. Kouba, S. Shanmughapriya, M. Potier-Cartereau, M. Trebak and N. Hempel, Mitochondrial Calcium Regulation of Redox Signaling in Cancer, *Cells*, 2020, **9**, 432.
13 M. J. Devine and J. T. Kittler, Mitochondria at the Neuronal Presynapse in Health and Disease, *Nat. Rev. Neurosci.*, 2018, **19**, 63–80.
14 K.-S. Lee, S. Huh, S. Lee, Z. Wu, A.-K. Kim, H.-Y. Kang and B. Lu, Altered ER-Mitochondria Contact Impacts Mitochondria Calcium Homeostasis and Contributes to Neurodegeneration in Vivo in Disease Models, *Proc. Natl. Acad. Sci. U. S. A.*, 2018, **115**, E8844–E8853.
15 E. Pchitskaya, E. Popugaeva and I. Bezprozvanny, Calcium Signaling and Molecular Mechanisms Underlying Neurodegenerative Diseases, *Cell Calcium*, 2018, **70**, 87–94.
16 E. Nam, J. Han, J.-M. Suh, Y. Yi and M. H. Lim, Link of Impaired Metal Ion Homeostasis to Mitochondrial Dysfunction in Neurons, *Curr. Opin. Chem. Biol.*, 2018, **43**, 8–14.
17 J. J. Woods and J. J. Wilson, Inhibitors of the Mitochondrial Calcium Uniporter for the Treatment of Disease, *Curr. Opin. Chem. Biol.*, 2020, **55**, 9–18.
18 A. De Mario, A. Tosatto, J. M. Hill, J. Kriston-Vizi, R. Ketteler, D. V. Reane, G. Cortopassi, G. Szabadkai, R. Rizzuto and C. Mammucari, Identification and Functional Validation of FDA-Approved Positive and Negative Modulators of the Mitochondrial Calcium Uniporter, *Cell Rep.*, 2021, **35**, 109275.
19 M. A. Matlib, Z. Zhou, S. Knight, S. Ahmed, K. M. Choi, J. Krause-Bauer, R. Phillips, R. Altschuld, Y. Katsube, N. Sperelakis and D. M. Bers, Oxygen-Bridged Dinuclear Ruthenium Amine Complex Specifically Inhibits Ca^{2+} Uptake into Mitochondria in Vitro and in Situ in Single Cardiac Myocytes, *J. Biol. Chem.*, 1998, **273**, 10223–10231.
20 J. Emerson, M. J. Clarke, W.-L. Ying and D. R. Sanadi, The Component of "Ruthenium Red" Responsible for Inhibition of Mitochondrial Calcium Ion Transport. Spectra, Electrochemistry, and Aquation Kinetics. Crystal Structure of μ-O-$[(HCO_2)(NH_3)_4Ru]_2Cl_3$, *J. Am. Chem. Soc.*, 1993, **115**, 11799–11805.
21 W.-L. Ying, J. Emerson, M. J. Clarke and D. R. Sanadi, Inhibition of Mitochondrial Calcium Ion Transport by an Oxo-Bridged Dinuclear Ruthenium Ammine Complex, *Biochemistry*, 1991, **30**, 4949–4952.
22 S. R. Nathan, N. W. Pino, D. M. Arduino, F. Perocchi, S. N. MacMillan and J. J. Wilson, Synthetic Methods for the Preparation of a Functional Analogue of Ru360, a Potent Inhibitor of Mitochondrial Calcium Uptake, *Inorg. Chem.*, 2017, **56**, 3123–3126.
23 J. Cervinka, A. Gobbo, L. Biancalana, L. Markova, V. Novohradsky, M. Guelfi, S. Zacchini, J. Kasparkova, V. Brabec and F. Marchetti, Ruthenium(II)–Tris-Pyrazolylmethane Complexes Inhibit Cancer Cell Growth by Disrupting Mitochondrial Calcium Homeostasis, *J. Med. Chem.*, 2022, **65**, 10567–10587.
24 J. J. Woods, N. Nemani, S. Shanmughapriya, A. Kumar, M. Zhang, S. R. Nathan, M. Thomas, E. Carvalho, K. Ramachandran, S. Srikantan, P. B. Stathopulos, J. J. Wilson and M. Madesh, A Selective and Cell-Permeable Mitochondrial Calcium Uniporter (MCU) Inhibitor Preserves Mitochondrial Bioenergetics after Hypoxia/Reoxygenation Injury, *ACS Cent. Sci.*, 2019, **5**, 153–166.
25 R. J. Novorolsky, M. Nichols, J. S. Kim, E. V. Pavlov, J. J. Woods, J. J. Wilson and G. S. Robertson, The Cell-Permeable Mitochondrial Calcium Uniporter Inhibitor Ru265 Preserves Cortical Neuron Respiration after Lethal Oxygen Glucose Deprivation and Reduces Hypoxic/Ischemic Brain Injury, *J. Cereb. Blood Flow Metab.*, 2020, **40**, 1172–1181.
26 J. J. Woods, J. Lovett, B. Lai, H. H. Harris and J. J. Wilson, Redox Stability Controls the Cellular Uptake and Activity of Ruthenium-Based Inhibitors of the Mitochondrial Calcium Uniporter (MCU), *Angew. Chem., Int. Ed.*, 2020, **59**, 6482–6491.
27 J. J. Woods, J. A. Spivey and J. J. Wilson, A $[^1H,^{15}N]$ Heteronuclear Single Quantum Coherence NMR Study of the Solution Reactivity of the Ruthenium-Based Mitochondrial Calcium Uniporter Inhibitor Ru265, *Eur. J. Inorg. Chem.*, 2022, **2022**, e202100995.
28 J. J. Woods, M. X. Rodriguez, C.-W. Tsai, M.-F. Tsai and J. J. Wilson, Cobalt Amine Complexes and Ru265 Interact with the DIME Region of the Mitochondrial Calcium Uniporter, *Chem. Commun.*, 2021, **57**, 6161–6164.
29 N. P. Bigham, Z. Huang, J. Spivey, J. J. Woods, S. N. MacMillan and J. J. Wilson, Carboxylate-Capped Analogues of Ru265 Are MCU Inhibitor Prodrugs, *Inorg. Chem.*, 2022, **61**, 17299–17312.
30 B. Testa, P. Crivori, M. Reist and P.-A. Carrupt, The Influence of Lipophilicity on the Pharmacokinetic Behavior of Drugs: Concepts and Examples, *Perspect. Drug Discovery Des.*, 2000, **19**, 179–211.
31 M. J. Waring, Defining Optimum Lipophilicity and Molecular Weight Ranges for Drug Candidates—Molecular Weight Dependent Lower Log D Limits Based on Permeability, *Bioorg. Med. Chem. Lett.*, 2009, **19**, 2844–2851.
32 X. Liu, B. Testa and A. Fahr, Lipophilicity and Its Relationship with Passive Drug Permeation, *Pharm. Res.*, 2011, **28**, 962–977.
33 T. W. Johnson, R. A. Gallego and M. P. Edwards, Lipophilic Efficiency as an Important Metric in Drug Design, *J. Med. Chem.*, 2018, **61**, 6401–6420.
34 M. Patra and G. Gasser, The Medicinal Chemistry of Ferrocene and Its Derivatives, *Nat. Rev. Chem.*, 2017, **1**, 0066.

35 K. Kowalski, Recent Developments in the Chemistry of Ferrocenyl Secondary Natural Product Conjugates, *Coord. Chem. Rev.*, 2018, **366**, 91–108.
36 B. Sharma and V. Kumar, Has Ferrocene Really Delivered Its Role in Accentuating the Bioactivity of Organic Scaffolds?, *J. Med. Chem.*, 2021, **64**, 16865–16921.
37 D. Dive and C. Biot, Ferrocene Conjugates of Chloroquine and Other Antimalarials: The Development of Ferroquine, a New Antimalarial, *ChemMedChem*, 2008, **3**, 383–391.
38 W. A. Wani, E. Jameel, U. Baig, S. Mumtazuddin and L. T. Hun, Ferroquine and Its Derivatives: New Generation of Antimalarial Agents, *Eur. J. Med. Chem.*, 2015, **101**, 534–551.
39 G. Jaouen, A. Vessières and S. Top, Ferrocifen Type Anti Cancer Drugs, *Chem. Soc. Rev.*, 2015, **44**, 8802–8817.
40 C. Biot, D. Taramelli, I. Forfar-Bares, L. A. Maciejewski, M. Boyce, G. Nowogrocki, J. S. Brocard, N. Basilico, P. Olliaro and T. J. Egan, Insights into the Mechanism of Action of Ferroquine. Relationship between Physicochemical Properties and Antiplasmodial Activity, *Mol. Pharm.*, 2005, **2**, 185–193.
41 D. Dive and C. Biot, Ferroquine as an Oxidative Shock Antimalarial, *Curr. Top. Med. Chem.*, 2014, **14**, 1684–1692.
42 S. Top, A. Vessières, C. Cabestaing, I. Laios, G. Leclercq, C. Provot and G. Jaouen, Studies on Organometallic Selective Estrogen Receptor Modulators (SERMs) Dual Activity in the Hydroxy-Ferrocifen Series, *J. Organomet. Chem.*, 2001, **637–639**, 500–506.
43 S. Top, A. Vessières, G. Leclercq, J. Quivy, J. Tang, J. Vaissermann, M. Huché and G. Jaouen, Synthesis, Biochemical Properties and Molecular Modelling Studies of Organometallic Specific Estrogen Receptor Modulators (SERMs), the Ferrocifens and Hydroxyferrocifens: Evidence for an Antiproliferative Effect of Hydroxyferrocifens on Both Hormone-Dependent and Hormone-Independent Breast Cancer Cell Lines, *Chem. – Eur. J.*, 2003, **9**, 5223–5236.
44 N. Chavain, H. Vezin, D. Dive, N. Touati, J.-F. Paul, E. Buisine and C. Biot, Investigation of the Redox Behavior of Ferroquine, a New Antimalarial, *Mol. Pharm.*, 2008, **5**, 710–716.
45 F. Dubar, C. Slomianny, J. Khalife, D. Dive, H. Kalamou, Y. Guérardel, P. Grellier and C. Biot, The Ferroquine Antimalarial Conundrum: Redox Activation and Reinvasion Inhibition, *Angew. Chem., Int. Ed.*, 2013, **52**, 7690–7693.
46 A. Vessières, C. Corbet, J. M. Heldt, N. Lories, N. Jouy, I. Laïos, G. Leclercq, G. Jaouen and R.-A. Toillon, A Ferrocenyl Derivative of Hydroxytamoxifen Elicits an Estrogen Receptor-Independent Mechanism of Action in Breast Cancer Cell Lines, *J. Inorg. Biochem.*, 2010, **104**, 503–511.
47 C. Lu, J.-M. Heldt, M. Guille-Collignon, F. Lemaître, G. Jaouen, A. Vessières and C. Amatore, Quantitative Analyses of ROS and RNS Production in Breast Cancer Cell Lines Incubated with Ferrocifens, *ChemMedChem*, 2014, **9**, 1286–1293.
48 A. van Niekerk, P. Chellan and S. F. Mapolie, Heterometallic Multinuclear Complexes as Anti-Cancer Agents-An Overview of Recent Developments, *Eur. J. Inorg. Chem.*, 2019, **2019**, 3432–3455.
49 J. A. Platts, S. P. Oldfield, M. M. Reif, A. Palmucci, E. Gabano and D. Osella, The RP-HPLC Measurement and QSPR Analysis of Log $P_{o/w}$ Values of Several Pt(II) Complexes, *J. Inorg. Biochem.*, 2006, **100**, 1199–1207.
50 I. V. Tetko, I. Jaroszewicz, J. A. Platts and J. Kuduk-Jaworska, Calculation of Lipophilicity for Pt(II) Complexes: Experimental Comparison of Several Methods, *J. Inorg. Biochem.*, 2008, **102**, 1424–1437.
51 M. H. M. Klose, S. Theiner, H. P. Varbanov, D. Hoefer, V. Pichler, M. Galanski, S. M. Meier-Menches and B. K. Keppler, Development and Validation of Liquid Chromatography-Based Methods to Assess the Lipophilicity of Cytotoxic Platinum(IV) Complexes, *Inorganics*, 2018, **6**, 130.
52 OECD, Test No. 117: Partition Coefficient (n-octanol/water), HPLC Method, **https://www.oecd-ilibrary.org/environment/test-no-117-partition-coefficient-n-octanol-water-hplc-method_9789264069824-en**, (accessed November 2022).
53 C. T. Chiou, V. H. Freed, D. W. Schmedding and R. L. Kohnert, Partition Coefficient and Bioaccumulation of Selected Organic Chemicals, *Environ. Sci. Technol.*, 1977, **11**, 475–478.
54 T. C. Johnstone and S. J. Lippard, The Effect of Ligand Lipophilicity on the Nanoparticle Encapsulation of Pt(IV) Prodrugs, *Inorg. Chem.*, 2013, **52**, 9915–9920.
55 F. A. Cotton and A. H. Reid Jr., Solid-State Structure of Ferrocenecarboxylic Acid, $[Fe(C_5H_4CO_2H)(C_5H_5)]$, *Acta Crystallogr., Sect. C: Cryst. Struct. Commun.*, 1985, **41**, 686–688.
56 Z. Wang, H. Deng, X. Li, P. Ji and J.-P. Cheng, Standard and Absolute pK_a Scales of Substituted Benzoic Acids in Room Temperature Ionic Liquids, *J. Org. Chem.*, 2013, **78**, 12487–12493.
57 T. Matsue, D. H. Evans, T. Osa and N. Kobayashi, Electron-Transfer Reactions Associated with Host-Guest Complexation. Oxidation of Ferrocenecarboxylic Acid in the Presence of β-Cyclodextrin, *J. Am. Chem. Soc.*, 1985, **107**, 3411–3417.
58 N. G. Connelly and W. E. Geiger, Chemical Redox Agents for Organometallic Chemistry, *Chem. Rev.*, 1996, **96**, 877–910.
59 N. Elgrishi, K. J. Rountree, B. D. McCarthy, E. S. Rountree, T. T. Eisenhart and J. L. Dempsey, A Practical Beginner's Guide to Cyclic Voltammetry, *J. Chem. Educ.*, 2018, **95**, 197–206.
60 M. B. Robin and P. Day, in *Advances in Inorganic Chemistry and Radiochemistry*, ed. H. J. Emeléus and A. G. Sharpe, Academic Press, New York, 1968, vol. 10, pp. 247–422.
61 P. Zanello, in *Inorganic Electrochemistry: Theory, Practice and Application*, Royal Society of Chemistry, Cambridge, 2003, pp. 171–182.

62 H. Masui and A. B. P. Lever, Correlations between the Ligand Electrochemical Parameter, $E_L(L)$, and the Hammett Substituent Parameter, σ, *Inorg. Chem.*, 1993, **32**, 2199–2201.

63 A. B. P. Lever, Electrochemical Parametrization of Metal Complex Redox Potentials, Using the Ruthenium(III)/Ruthenium(II) Couple To Generate a Ligand Electrochemical Series, *Inorg. Chem.*, 1990, **29**, 1271–1285.

64 P. E. Hoggard, in *Optical Spectra and Chemical Bonding in Inorganic Compounds. Structure and Bonding*, ed. D. M. P. Mingos and T. Schönherr, Springer, Berlin, Heidelberg, 2004, vol. 106, pp. 37–57.

65 F. Dubar, G. Anquetin, B. Pradines, D. Dive, J. Khalife and C. Biot, Enhancement of the Antimalarial Activity of Ciprofloxacin Using a Double Prodrug/Bioorganometallic Approach, *J. Med. Chem.*, 2009, **52**, 7954–7957.

66 T. Stringer, D. Taylor, C. De Kock, H. Guzgay, A. Au, S. H. An, B. Sanchez, R. O'Connor, N. Patel, K. M. Land, P. J. Smith, D. T. Hendricks, T. J. Egan and G. S. Smith, Synthesis, Characterization, Antiparasitic and Cytotoxic Evaluation of Thioureas Conjugated to Polyamine Scaffolds, *Eur. J. Med. Chem.*, 2013, **69**, 90–98.

67 A. Minta, J. P. Y. Kao and R. Y. Tsien, Fluorescent Indicators for Cytosolic Calcium Based on Rhodamine and Fluorescein Chromophores, *J. Biol. Chem.*, 1989, **264**, 8171–8178.

68 J. J. Woods, R. J. Novorolsky, N. P. Bighman, G. S. Robertson and J. J. Wilson, Dinuclear Nitrido-Bridged Osmium Complexes Inhibit the Mitochondrial Calcium Uniporter and Protect Cortical Neurons Against Lethal Oxygen-Glucose Deprivation, *RSC Chem. Biol.*, 2022, DOI: **10.1039/D2CB00189F**.